

# Scanning tunneling spectroscopy of a magnetic atom on graphene in the Kondo regime

Huai-Bin Zhuang<sup>1</sup>, Qing-feng Sun<sup>1</sup>, and X. C. Xie<sup>1,2</sup>

<sup>1</sup>*Beijing National Lab for Condensed Matter Physics and Institute of Physics, Chinese Academy of Sciences, Beijing 100190, China*

<sup>2</sup>*Department of Physics, Oklahoma State University, Stillwater, Oklahoma 74078*

(Dated: June 21, 2021)

The Kondo effect in the system consisting of a magnetic adatom on the graphene is studied. By using the non-equilibrium Green function method with the slave-boson mean field approximation, the local density of state (LDOS) and the conductance are calculated. For a doped graphene, the Kondo phase is present at all time. Surprisingly, two kinds of Kondo regimes are revealed. But for the undoped graphene, the Kondo phase only exists if the adatom's energy level is beyond a critical value. The conductance is similar to the LDOS, thus, the Kondo peak in the LDOS can be observed with the scanning tunneling spectroscopy. In addition, in the presence of a direct coupling between the STM tip and the graphene, the conductance may be dramatically enhanced, depending on the coupling site.

PACS numbers: 81.05.Uw, 72.15.Qm

Graphene, a single-layer hexagonal lattice of carbon atoms, has recently attracted a great deal of attention due to its unique properties and potential applications.<sup>1,2</sup> The graphene has a unique band structure with a linear dispersion near the Dirac-points, such that its quasi-particles obey the two-dimensional Dirac equation and have the relativistic-like behaviors. For a neutral graphene, the Fermi level passes through the Dirac points and the density of states (DOS) at the Fermi face vanishes, so that its transport properties are greatly deviated from that of a normal metal.

The Kondo effect has been paid great attention in condensed matter community over the years.<sup>3,4,5</sup> It is a prototypical many-body correlation effect involving the interaction between a localized spin and free electrons. The Kondo effect occurs in the system of a magnetic impurity embedded in a metal<sup>3,4,5</sup> or a quantum dot coupled to the leads,<sup>6,7,8</sup> in which the magnetic impurity or the quantum dot acts as a localized spin. At low temperature, the localized spin is screened by the free electrons, resulting a spin singlet and a very narrow Kondo peak located near the Fermi surface in the local DOS (LDOS).

For a conventional metal, it has a finite DOS at the Fermi surface, thus, at zero temperature the Kondo effect can occur with any weak exchange interaction  $J_{ex}$  between the magnetic impurity and the free electrons. But in certain special systems, such as the nodal d-wave superconductors or the Luttinger liquids, the DOS vanishes at the Fermi surface with power law behavior. In these systems, there exists a critical exchange coupling  $J_c$ , and the Kondo effect only occurs when the exchange interaction  $J_{ex} > J_c$ .<sup>9</sup>

The graphene, which was successfully fabricated in recent years, has an unique band structure.<sup>1</sup> For the undoped neutral graphene, its DOS is directly proportional to the energy  $|\epsilon|$  and the DOS vanishes at the Fermi surface, so it has an unconventional Kondo effect. Very recently, some studies have investigated the Kondo effect in the graphene and a finite critical Kondo coupling

strength was revealed.<sup>10,11</sup> By varying the gate voltage, the charge carriers of graphene can be easily tuned experimentally. Then the Fermi level can be above or below the Dirac points, and the DOS depends on the energy  $\epsilon$  in the form  $|\epsilon - \epsilon_0|$ , with the Dirac-point energy denoted by  $\epsilon_0$ . In this situation, the DOS is quite small but finite at the Fermi surface. In addition, there exists a zero point in DOS that is very close to the Fermi surface. How is the Kondo effect affected by this unique energy band structure?

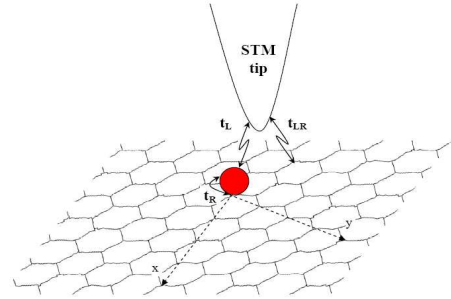


FIG. 1: (Color online) The schematic diagram for a magnetic adatom on the graphene probed by a STM tip.

In this Letter, we study the Kondo effect in the graphene. We consider the model of a magnetic adatom on the graphene and to investigate its scanning tunneling spectroscopy by attaching a STM tip near the magnetic adatom (see Fig.1). Taking the slave-boson (SB) mean field approximation and using the non-equilibrium Green function method, the expressions of the LDOS and conductance are obtained. Our results exhibit that for the doped graphene the Kondo phase always exists, however, two kinds of Kondo regimes emerge. For the undoped neutral graphene, the Kondo phase only exists when the energy level  $\epsilon_d$  of the adatom is larger than a critical value  $\epsilon_{dc}$ .

The above mentioned system can be described by the Anderson Hamiltonian. Here the magnetic atom is mod-

eled by a single level  $\epsilon_d$  with the spin index  $\sigma = \uparrow, \downarrow$  and a constant on-site Coulomb interaction  $U$ . In the limit  $U \rightarrow \infty$ , the double occupancy is forbidden. Then the SB representation can be applied, and the Hamiltonian of the Anderson model describing the system is transformed to the following form:<sup>12</sup>

$$\begin{aligned}
H = & \sum_{\sigma} \epsilon_d \hat{n}_{\sigma} + \sum_{i,\sigma} \epsilon_0 a_{i\sigma}^{\dagger} a_{i\sigma} + t \sum_{\langle ij \rangle, \sigma} a_{i\sigma}^{\dagger} a_{j\sigma} \\
& + \sum_{k,\sigma} \epsilon_k c_{k\sigma}^{\dagger} c_{k\sigma} + \sum_{k,\sigma} \left( t_L c_{k\sigma}^{\dagger} f_{\sigma} b^{\dagger} + t_{LR} c_{k\sigma}^{\dagger} a_{J\sigma} + H.c. \right) \\
& + \sum_{\sigma} \left( t_R f_{\sigma}^{\dagger} b a_{0\sigma} + H.c. \right) + \lambda (b^{\dagger} b + \sum_{\sigma} \hat{n}_{\sigma} - 1) \quad (1)
\end{aligned}$$

where  $\hat{n}_{\sigma} = f_{\sigma}^{\dagger} f_{\sigma}$ .  $a_{i\sigma}$  and  $c_{k\sigma}$  are the annihilation operators at the discrete site  $i$  of the graphene and the tip of STM, respectively. Here the graphene is assumed to be two-dimensional and without disorder. In Hamiltonian (1), the graphene is described by the tight-binding model and only the nearest neighbor hopping  $t$  is considered.  $f_{\sigma}$  and  $b$  are the pseudofermion operator and SB operator of the magnetic atom. The last term represents the single-occupancy constraint  $b^{\dagger} b + \sum_{\sigma} \hat{n}_{\sigma} = 1$  with Lagrange multiplier  $\lambda$ . The magnetic atom couples to the graphene at the lattice site 0 with the coupling coefficient  $t_R$ . The STM tip couples to both of the magnetic atom and graphene, and  $t_L$  and  $t_{LR}$  are their coupling coefficients. Here we consider that the STM tip only contacts to a lattice site  $J$  of the graphene. Following, we take the standard SB mean field approximation in which the operator  $b$  is replaced by the c-number  $\langle b \rangle$ . This approximation is a qualitative correct for describing the Kondo regime at zero temperature.<sup>12</sup> For convenience, we also introduce the renormalized energy  $\tilde{\epsilon}_d \equiv \epsilon_d + \lambda$  and hopping elements  $\tilde{t}_L \equiv t_L \langle b \rangle$  and  $\tilde{t}_R \equiv t_R \langle b \rangle$ .

Next, we consider that a bias  $V$  is applied between the STM tip and the graphene to obtain the current  $I$  flowing from STM to the graphene and the LDOS around the magnetic atom. By using the non-equilibrium Green function method, the current  $I$  and LDOS are:<sup>13</sup>

$$I = \frac{4e}{h} \int d\omega \mathbf{Re} \left[ \tilde{t}_L G_{fL}^{<}(\omega) + t_{LR} G_{JL}^{<}(\omega) \right], \quad (2)$$

$$\text{LDOS}(\omega) = -(1/\pi) \mathbf{Im} G_{ff}^r(\omega), \quad (3)$$

where  $\mathbf{G}^{<}$  and  $\mathbf{G}^r$  are the standard lesser and retarded Green's functions, and  $G_{ff/fL/JL}^{</r}$  in Eq.(2) and (3) are the elements of the matrix  $\mathbf{G}^{</r}$ . Under the SB mean field approximation,  $\mathbf{G}^{<}$  and  $\mathbf{G}^r$  can be solved from the Keldysh and Dyson equations:  $\mathbf{G}^{<} = (1 + \mathbf{G}^r \mathbf{\Sigma}^r) \mathbf{g}^{<}$  ( $1 + \mathbf{\Sigma}^a \mathbf{G}^a$ ) and  $\mathbf{G}^r = (\mathbf{g}^r - \mathbf{\Sigma}^r)^{-1}$ , where  $\mathbf{\Sigma}^{r,a}$  are the self-energies.  $\Sigma_{Lf}^r = \Sigma_{fL}^r = \tilde{t}_L$ ,  $\Sigma_{f0}^r = \Sigma_{0f}^r = \tilde{t}_R$ ,  $\Sigma_{LJ}^r = \Sigma_{JL}^r = t_{LR}$ , and other elements of  $\mathbf{\Sigma}^r$  are zero.  $\mathbf{g}^{r/<}$  are the Green's functions of the isolated STM tip, magnetic atom, and graphene (i.e. while  $\tilde{t}_L = \tilde{t}_R = t_{LR} = 0$ ). They can easily be obtained:  $g_{LL}^r(\omega) = \sum_k g_k^r = -i\pi\rho_L$ ,  $g_{ff}^r(\omega) = 1/(\omega - \tilde{\epsilon}_d + i0^+)$ ,  $g_{LL}^{<}(\omega) =$

$\sum_k g_k^{<} = 2i\pi\rho_L f_L(\omega)$ ,  $\mathbf{g}_{ij}^{<}(\omega) = -f_R(\omega)(\mathbf{g}_{ij}^r - \mathbf{g}_{ij}^a)$ , and

$$\begin{aligned}
\mathbf{g}_{ij}^r(\omega) = & \int \int dk_x dk_y e^{ia[(i_x - j_x)k_x + (i_y - j_y)k_y]} \mathbf{g}_{k_x k_y}^r(\omega) \\
\mathbf{g}_{k_x k_y}^r(\omega) = & \frac{1}{(\omega - \epsilon_0)^2 - |\phi|^2} \begin{pmatrix} \omega - \epsilon_0 & \phi \\ \phi^* & \omega - \epsilon_0 \end{pmatrix}, \quad (5)
\end{aligned}$$

where  $\rho_L$  is the DOS of the STM tip.  $f_L(\omega)$  and  $f_R(\omega)$  are the Fermi-Dirac distribution functions in the isolated STM tip and graphene, respectively.  $\mathbf{g}_{ij}^{r/<}(\omega)$  are the Green's functions of the isolated graphene, and  $\mathbf{i} = (i_x, i_y)$  and  $\mathbf{j} = (j_x, j_y)$  are the indices of the unit cell. Since there are two carbon atoms per unit cell,  $\mathbf{g}_{ij}^r$  is a  $2 \times 2$  matrix. In Eq.(4) and (5),  $a$  is the lattice constant of the graphene, the integral  $dk_x dk_y$  runs over the first Brillouin zone, and  $\phi = t(1 + e^{-iak_x} + e^{-iak_x + iak_y})$ .

At end we need to self-consistently calculate two unknowns  $\langle b \rangle$  and  $\lambda$  with the self-consistent equations:

$$\langle b \rangle^2 + n_{\uparrow} + n_{\downarrow} = 1 \quad (6)$$

$$2Im \int \frac{d\omega}{2\pi} \left( \tilde{t}_L G_{LJ}^{<}(\omega) + \tilde{t}_R G_{0J}^{<}(\omega) \right) + \lambda \langle b \rangle^2 = 0 \quad (7)$$

where  $n_{\sigma} = \int (d\omega/2\pi) Im G_{ff}^{<}(\omega)$  is the electron occupation number in the spin state  $\sigma$  of the magnetic atom. In the numerical calculations, we take the hopping energy  $t = 1$  as the energy unit. The chemical potential  $\mu_R$  of the graphene is set to be zero as the energy zero point, then the bias voltage  $V = \mu_L$ . The temperature  $T$  is assumed to be zero since  $k_B T$  is much smaller than  $t = 2.75eV$  in the real experiments.

First, we assume the system to be decoupled to the STM tip (i.e. at  $t_L = t_{LR} = 0$ ) and focus on the Kondo effect. Fig.2 shows magnetic-atom LDOS for different  $\epsilon_d$  and  $\epsilon_0$ . Here the Dirac-point energy  $\epsilon_0$  can be experimentally tuned by the gate voltage. For the magnetic atom, the level  $\epsilon_d$  is fixed. But for an artificial atom, such as a quantum dot,  $\epsilon_d$  is also tunable.<sup>8</sup> As shown in Fig.2a, there exists three peaks in the LDOS. Two peaks locate at  $\omega = \pm t$ , due to the peaks in the DOS of the graphene. The third peak is the Kondo peak, which is always located around  $\mu_R = 0$  regardless of the parameters of  $\epsilon_d$ ,  $\epsilon_0$ , and  $t_R$ . Fig.2b magnifies the curves of Fig.2a in the vicinity of  $\omega = 0$ . It clearly shows that the Kondo peak is much higher than the other two peaks at  $\omega = \pm t$ . The lower the level  $\epsilon_d$  is, the higher and sharper is the Kondo peak and the closer it is to  $\mu_R = 0$ . In particular, for the undoped neutral graphene with  $\epsilon_0 = 0$ , the Kondo peak is greatly deflected from 0 (see Fig.2b) although it seems to be near 0 on a large scale (see Fig.2a). The LDOS is zero at  $\omega = 0$  since the graphene's DOS vanishes at this point. This characteristics is much different from the conventional Kondo effect, in which the LDOS is quite large at  $\omega = 0$ .

Next, the energy  $\epsilon_0$  is tuned to be away from zero. While  $\epsilon_0 < 0$ , the carriers in graphene are electron-like, but they are hole-like for  $\epsilon_0 > 0$ . With  $\epsilon_0$  decreasing from 0, the Kondo peak is gradually getting closer to

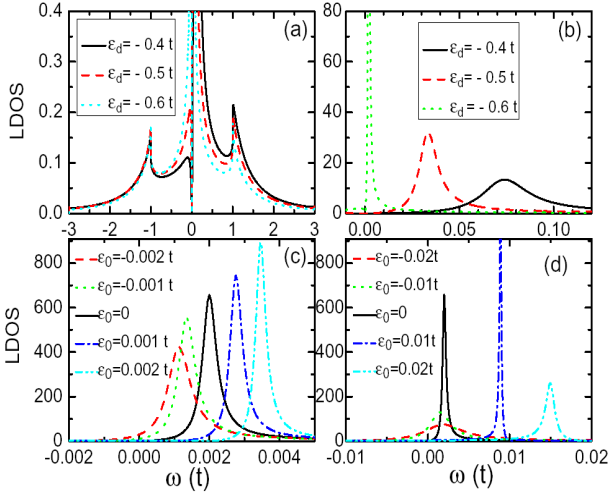


FIG. 2: (Color online) LDOS vs. the energy  $\omega$  with  $t_L = t_{LR} = 0$  and  $t_R = 0.9t$ . In (a), the Dirac-point energy  $\epsilon_0 = 0$ . (b) is the enlarged view of the Kondo peaks in (a). (c) and (d) are at different  $\epsilon_0$  for the level  $\epsilon_d = -0.6t$ .

0 and is slightly widened (see Fig.2c). It recovers the shape of conventional Kondo peak at large negative  $\epsilon_0$  (e.g.  $\epsilon_0 = -0.01t$  or  $-0.02t$  in Fig.2d). On the other hand, with  $\epsilon_0$  increasing from 0, the Kondo peak departs gradually from 0 and its shape never recovers to that of the conventional Kondo peak even at large  $\epsilon_0$ .

From the position  $\omega_1$  and half-width  $\tilde{\Gamma}_R$  of the Kondo peak, we can estimate the Kondo temperature by<sup>4</sup>  $T_k = \sqrt{\omega_1^2 + \tilde{\Gamma}_R^2}(\omega_1)$ , where the peak position  $\omega_1$  is obtained from the equation  $\omega - \tilde{\epsilon}_d - \text{Re}[t_R^2 g_{00}^r(\omega)] = 0$  and the peak half-width  $\tilde{\Gamma}_R = -2t_R^2 \text{Im}[g_{00}^r(\omega)]$ . Fig.3a shows the Kondo temperature  $T_k$  versus the level  $\epsilon_d$  at a fixed  $t_R$  for different energy  $\epsilon_0$ .  $T_k$  possesses the following characteristics: (i)  $T_k$  decreases monotonically with reducing of  $\epsilon_d$ . When  $\epsilon_d$  is approaching  $-\infty$ ,  $T_k$  goes to zero. (ii) For  $\epsilon_0 \neq 0$ , there exists two different Kondo regimes. When  $\epsilon_d$  is larger than a critical value  $\epsilon_{dc}$ ,  $T_k$  is almost linearly dependent on  $\epsilon_d - \epsilon_{dc}$ , so that  $T_k$  drops rapidly while  $\epsilon_d$  is near  $\epsilon_{dc}$  (see Fig.3a). This characteristics is very different comparing to the conventional Kondo effect, and it origins from the linear DOS of the graphene and vanish-ness of the DOS at the Dirac point. On the other hand, when  $\epsilon_d < \epsilon_{dc}$ ,  $T_k \propto e^{\epsilon_d}$  (i.e.  $\ln T_k \propto \epsilon_d$  as shown in Fig.3a). In this case the system's behavior is similar to that of the conventional Kondo effect. Since  $k_B T_k \ll |\epsilon_0 - \mu_R|$  in this regime, the DOS at the Fermi surface is approximatively constant on the energy scale  $k_B T_k$ . So it recovers the conventional Kondo behavior. (iii) The behavior of  $T_k$  for  $\epsilon_0 < 0$  (i.e. the electron doped graphene) and  $\epsilon_0 > 0$  (i.e. the hole doped graphene) is similar.

Fig.3b shows the renormalized level  $\tilde{\epsilon}_d$  which determines the position of the Kondo peak. While  $\epsilon_0 < 0$ , the renormalized level  $\tilde{\epsilon}_d$  is always positive and it decreases monotonically with reducing of  $\epsilon_d$ .  $\tilde{\epsilon}_d$  approaches zero as

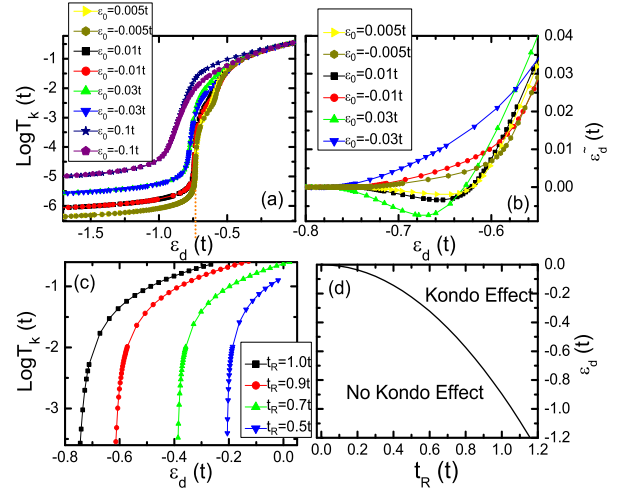


FIG. 3: (Color online) (a)  $T_k$  vs. the level  $\epsilon_d$  and (b)  $\tilde{\epsilon}_d$  vs.  $\epsilon_d$  at  $t_R = 0.9t$  for different energy  $\epsilon_0$ . (c)  $T_k$  as functions of  $\epsilon_d$  for  $\epsilon_0 = 0$  at different coupling  $t_R$ . (d) Phase diagram of the  $\epsilon_0 = 0$  in the parameter space of  $(\epsilon_d, t_R)$ .

$\epsilon_d \rightarrow -\infty$ . On the other hand, while  $\epsilon_0 > 0$ ,  $\tilde{\epsilon}_d$  can be negative. The curve of  $\tilde{\epsilon}_d - \epsilon_d$  has a negative minimum. But  $\tilde{\epsilon}_d \rightarrow 0$  is still true as  $\epsilon_d \rightarrow -\infty$ .

Now we focus on the case of  $\epsilon_0 = 0$ . When the Dirac-point energy  $\epsilon_0$  approaches to 0, the zero-DOS point approaches to the Fermi surface, then both of the Kondo temperature  $T_k$  and the renormalized level  $\tilde{\epsilon}_d$  go to zero in the whole region of  $\epsilon_d < \epsilon_{dc}$ . At  $\epsilon_0 = 0$  (i.e. for the undoped neutral graphene),  $T_k$  and  $\tilde{\epsilon}_d$  reach zero at  $\epsilon_d = \epsilon_{dc}$ . On the  $\epsilon_d < \epsilon_{dc}$  side, the self-consistent equations (6) and (7) do not have a solution. In other words, the system cannot be in the Kondo phase for  $\epsilon_d < \epsilon_{dc}$ . On the other side with  $\epsilon_d > \epsilon_{dc}$ , the Kondo phase does exist. The Kondo temperature  $T_k$  is roughly proportional to  $\epsilon_d - \epsilon_{dc}$  (see Fig.3c). The critical value  $\epsilon_{dc}$  depends on the coupling strength  $t_R$  between the magnetic atom and the graphene. The larger  $t_R$  is, the larger  $|\epsilon_{dc}|$  is (see Fig.3c). From  $T_k = 0$  or  $\tilde{\epsilon}_d = 0$  at  $\epsilon_d = \epsilon_{dc}$  and with the aid of Eq.(7), the critical value  $\epsilon_{dc}$  can be analytically obtained:

$$\epsilon_{dc} = -\frac{2}{\pi} t_R^2 \int_{-\infty}^0 d\omega \frac{\text{Im}(g_{II}^r(\omega))}{\omega} \quad (8)$$

The above integral over  $\omega$  is about 1.408, hence  $\epsilon_{dc} \approx 0.896 t_R^2$ . Fig.3d shows the phase diagram in the parameter space of  $(\epsilon_d, t_R)$ . The curve gives the critical value  $\epsilon_{dc}$  versus the coupling strength  $t_R$ . In the top right region, the Kondo phase emerges at low temperature. But in the bottom left region, the system cannot enter into the Kondo state even at zero temperature.

Finally, we investigate the conductance  $G$  ( $G \equiv dI/dV$ ) while the STM tip is coupled. The coupling between the STM tip and the adatom is normally much weak compared to that between the graphene to the adatom, so we set  $t_L$  and  $t_{LR}$  on the order of  $0.01t$ . Fig.4

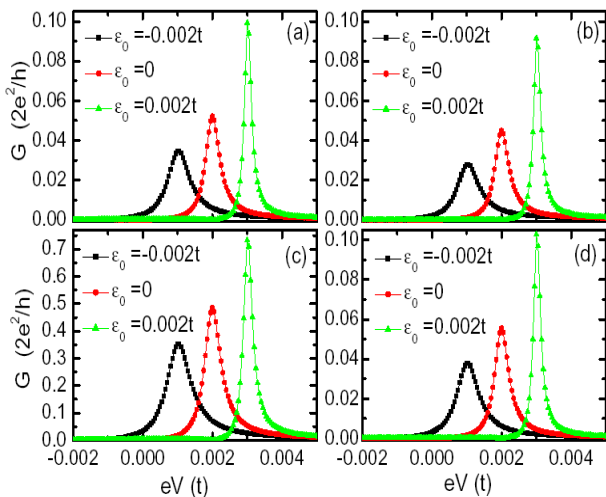


FIG. 4: (Color online) Conductance  $G$  vs. the bias  $V$  for different energy  $\epsilon_0$  with  $t_R = 0.9t$ ,  $t_L = 0.002t$ , and  $\epsilon_d = -0.6t$ . In (a),  $t_{LR} = 0$ , and in (b), (c), and (d),  $t_{LR} = 0.03t$ . The contact point  $J$  of the STM tip and the graphene in (b), (c), and (d) are 0, 1, and 2, respectively.

shows the conductance  $G$  versus the bias  $V$  in the Kondo regime. While without the direct coupling ( $t_{LR} = 0$ ), the curve of  $G$ - $V$  is very similar to the curve of LDOS- $\omega$  (see Fig.4a and 2c) since for the weak-coupled STM tip, the conductance  $G$  is proportional to the LDOS of the adatom.<sup>14</sup> When the direct coupling is present ( $t_{LR} \neq 0$ ), the coherence between the direct path and the path passing the magnetic adatom occurs, which usually leads to the Fano resonance.<sup>15</sup> But in the present graphene system, the Fano resonance does not appear anywhere, the reason is that the transmission coefficient of the direct path also depends on the energy of the incident electron. In Fig.4b, 4c, and 4d,  $J$  of the contact point of the STM tip to the graphene is 0 (same contact point with the adatom), 1 (the nearest neighbor site), and 2 (the next

nearest neighbor site), respectively. For the same and the next nearest neighbor contact points, the conductance  $G$  is almost unaffected by the opening of the direction path, although  $t_{LR} = 0.03t$  is much larger than  $t_L = 0.002t$ . Because that in the Kondo regime, a high Kondo peak emerges in the LDOS of the adatom, so the path passing the adatom is large and plays the dominant role. However, when the contact point is at the nearest neighbor site, the conductance is greatly enhanced by the opening of the direct path (see Fig.4c, note the different scale comparing with the other plots in Fig.4) since the Kondo singlet state is quite extensive. For the graphene system, the sharp Kondo peak not only appears in the LDOS of the adatom, but also in the LDOS of all odd-neighboring sites. The large LDOS in the odd-neighboring sites and  $t_{LR} > t_L$  lead that the direct path is dominant, and the conductance  $G$  is enhanced.

In summary, the Kondo effect in the system of a magnetic adatom on the graphene and its scanning tunneling spectroscopy are theoretically studied. For a doped graphene, the Kondo phase always exists at zero temperature regardless of  $n$ -type or  $p$ -type doping, and it exhibits two Kondo regimes: the conventional and unconventional. For the undoped neutral graphene, the Kondo phase only exists while the adatom's energy level is above a critical value. These Kondo characteristics can be observed from scanning tunneling spectroscopy since the conductance versus the bias is similar to the LDOS of the adatom. In addition, if a direct coupling between the STM tip and the graphene is present, the conductance may be greatly enhanced, depending on the coupling site.

**Acknowledgments:** We gratefully acknowledge the financial support from NSF-China under Grants Nos. 10525418 and 10734110, National Basic Research Program of China (973 Program project No. 2009CB929103), and US-DOE under Grants No. DE-FG02-04ER46124.

<sup>1</sup> K.S. Novoselov, *et al.*, Science **306**, 666 (2004); Nature (London) **438**, 197 (2005); Y. Zhang, *et al.*, Nature (London) **438**, 201 (2005).  
<sup>2</sup> C.W.J. Beenakker, Rev. Mod. Phys. **80**, 1337 (2008); A.H. Castro Neto, *et al.*, arXiv:0709.1163 (2007).  
<sup>3</sup> J. Kondo, Prog. Theor. Phys. **32**, 37 (1964).  
<sup>4</sup> A.C. Hewson, *the Kondo problem to heavy Fermions* (Cambridge University Press, Cambridge, UK, 1993).  
<sup>5</sup> K.G. Wilson, Rev. Mod. Phys. **47**, 773 (1975).  
<sup>6</sup> T.K. Ng and P.A. Lee, Phys. Rev. Lett. **61**, 1768 (1988).  
<sup>7</sup> Y. Meir, N.S. Wingreen, and P.A. Lee, Phys. Rev. Lett. **70** 2601 (1993).  
<sup>8</sup> S.M. Cronenwett, *et al.*, Science **281**, 540 (1998); T. Inoshita, Science **281**, 526 (1998); D. Goldhaber-Gordon *et al.*, Nature (London) **391**, 156 (1998); W.G. van der Wiel *et al.*, Science **289**, 2105 (2000).  
<sup>9</sup> D. Withoff and E. Fradkin, Phys. Rev. Lett. **64**, 1853

(1990); K. Ingersent, Phys. Rev. B **54**, 11936 (1996).  
<sup>10</sup> M. Hentschel and F. Guinea, Phys. Rev. B **76**, 115407 (2007); B. Dora and P. Thalmeier, *ibid.* **76**, 115435 (2007).  
<sup>11</sup> K. Sengupta and G. Baskaran, Phys. Rev. B **77**, 045417 (2008).  
<sup>12</sup> R. Aguado and D.C. Langreth, Phys. Rev. Lett. **85**, 1946 (2000); H. Hu, G.M. Zhang, and L. Yu, *ibid.* **86**, 5558 (2001).  
<sup>13</sup> Y. Meir and N.S. Wingreen, Phys. Rev. Lett. **68**, 2512 (1992).  
<sup>14</sup> Q.-f. Sun and H. Guo, Phys. Rev. B **64**, 153306 (2001); E. Lebanon and A. Schiller, *ibid.* **65**, 035308 (2001); S. De Franceschi, *et al.*, Phys. Rev. Lett. **89**, 156801 (2002).  
<sup>15</sup> B.R. Bulka and P. Stefanski, Phys. Rev. Lett. **86**, 5128 (2001); W. Hofstetter, J. König, and H. Schoeller, *ibid.* **87**, 156803 (2001).